FULL TITLE OF MANUSCRIPT: Whole-body MRI Quantification for Assessment of Bone Lesions in CNO Patients Treated with Pamidronate: A Prevalence, Reproducibility, and Responsiveness Study

AUTHORS: Jyoti Panwar[1,2]; Mirkamal Tolend[2]; Lillian Lim[3]; Shirley M. Tse[4]; Andrea S. Doria[2]; Ronald M. Laxer[4]; Jennifer Stimec[2].

AUTHOR AFFILIATIONS:

[1]Department of Radiodiagnosis, Christian Medical College and Hospital, Vellore, India;

[2] Department of Diagnostic Imaging, The Hospital for Sick Children, Department of Medical Imaging, University of Toronto, Toronto, ON, Canada;

[3]Division of Pediatric Rheumatology, Department of Pediatrics, University of Alberta; Edmonton, AB, Canada;

[4]Division of Rheumatology, The Hospital for Sick Children, University of Toronto, Toronto, ON, Canada

CORRESPONDING AUTHOR: Jyoti Panwar, MD, FRCR, Professor, Department of Radiodiagnosis, Christian Medical College and Hospital, Vellore, India, Phone: +91-638-5209-311. Department of Diagnostic Imaging, The Hospital for Sick Children, Department of Medical Imaging, University of Toronto, Toronto, ON, Canada

Email: drjyoticmch@gmail.com, jyoti.panwar@sickkids.ca

AUTHOR CONTRIBUTIONS:

Stimec J, Panwar J. conceived and designed the study.

Panwar J and Stimec J have analyzed and interpreted the whole-body MRI studies.

Panwar J, Tolend M have collected and archived most of the images and prepared tables used in the study.

Lim L has collected details of the clinical measures including demographic details.

Tolend M has performed the statistical analysis.

All authors contributed to the discussion of the various points shown in this work, critically reviewed the manuscript for important intellectual content, and approved the final version for publication.

Panwar J. wrote up the first manuscript draft.

RUNNING TITLE: WB-MRI Scoring System in Pediatric CNO.

THE SOURCE OF SUPPORT: None

ABSTRACT:

Objective:

The purpose of this study was 1) to assess the inter-reader reliability in detecting and scoring the inflammatory bone lesions in pediatric patients with chronic nonbacterial osteomyelitis (CNO) by using WB-MRI, and 2) to evaluate the responsiveness of the MRI-detected CNO lesions to pamidronate therapy.

Methods:

Eighty-eight WB-MRI examinations were independently reviewed and scored by two radiologists blinded to clinical details in 32 retrospectively enrolled pediatric patients with CNO. Inflammatory bone lesions, soft tissue abnormality, and bony structural changes were scored before and after pamidronate therapy. Lesion responsiveness was calculated by using standardized response mean and inter-reader reliability was assessed by kappa statistics.

Results:

There was good to excellent inter-reader agreement for the detection and quantification of bone lesions. After the first cycle of pamidronate in all 32 patients, 96 of the 279 lesions (34%) (after excluding 108 lesions of hand and feet) resolved, while in a subset of 11 patients with two or more cycles, 76% of lesions resolved after the second cycle. Twenty-one (7.5%) lesions worsened and 46 (16.4%) new lesions developed after one cycle in all 32 patients. In these 11 patients, the number of worsened lesions reduced to 2 (2%) and new lesions to 14 (14.9%) after the second cycle as detected on MRI. Vertebral lesions had the highest response to treatment.

Conclusions:

WB-MRI is a reliable tool for objective quantification and assessment of response to treatment of pediatric CNO bone lesions and could be used to monitor disease activity for clinical and research purposes.

KEY INDEXING TERMS: Pediatric, chronic recurrent multifocal osteomyelitis, chronic nonbacterial osteomyelitis, magnetic resonance imaging, scoring system, reliability/ reproducibility of results, responsiveness, pamidronate.

INTRODUCTION:

Chronic nonbacterial osteomyelitis (CNO), also known as chronic recurrent multifocal osteomyelitis, is a rare inflammatory bone disorder characterized by relapsing and remitting aseptic bone lesions[1,2]. It occurs primarily in children and adolescents who present with recurrent nonspecific osseous pain and swelling and may sometimes be associated with systemic symptoms such as fever,

weight loss, and generalized malaise[3,4]. The median age of disease onset is 10 years with a predilection for females[5]. The etiology remains unclear and is presumed to be an autoinflammatory disorder[2,6]. It can be associated with SAPHO syndrome[6], inflammatory bowel disease[7], psoriasis[8], and sacroiliitis[9,10]. CNO usually affects the metaphysis of tubular bones, mainly the lower extremities, followed by the clavicle and spine[11-13]. Several imaging methods can be used to assess CNO lesions including radiographs, computed tomography, MRI, and bone scintigraphy[14,15]. MRI is more sensitive than radiographs in the early detection of bone and soft tissue inflammatory lesions of CNO, which is important for diagnosis and institution of appropriate management to ensure improved patient outcomes and quality of life[16].

Approximately 80% of patients respond to treatment with non-steroidal anti-inflammatory drugs (NSAIDs)[17-19] and the remainder may be treated with second-line therapy including sulfasalazine, methotrexate[17,19], corticosteroids[17,19], bisphosphonates[20,21,] and biologic agents[18,21,22]. Fluid sensitive fat-saturated whole-body (WB)-MRI sequences are highly sensitive and specific in demonstrating active disease along with the extent of the lesions and are proved to be very effective for initial and follow-up diagnostics for children with CNO[23-26]. There have only been a few studies that have evaluated the treatment response of patients with CNO on WB-MRI[26-31] or the efficacy of pamidronate as second-line therapy of CNO[27-31]. Despite the frequent application of WB-MRI in the assessment of CNO lesions, there is only one recent consensus-driven study published regarding the comprehensive quantification of disease by scoring these bone lesions and evaluating the interrater reliability[32]. There is no published study compared to the total skeleton disease load pre- and post-treatment by using the WB-MRI grading and scoring system. Hence, this study attempted to evaluate the inter-observer reliability and to assess the response to pamidronate in pediatric CNO by utilizing the WB-MRI quantification system.

METHODS:

This retrospective study was undertaken at a large pediatric quaternary care referral center and approved by the institutional research ethics board (REB no. 1000044463). The consent from all patients was waived owing to the retrospective features of the study. WB-MRI is a routine investigation at our institution utilized for initial diagnosis and follows up to evaluate the effect of drug therapy on pediatric CNO lesions.

Patient Selection:

The patients identified and included in the study were all under the age of 18 years, had a clinical (fulfilling the Bristol Criteria)[33,34] and/or biopsy-proven diagnosis of CNO, was followed in the Rheumatology Clinic at The Hospital for Sick Children, and underwent pre and post pamidronate WB-MRI examinations within a period of 12 months from May 2010 to June 2017. WB-MRIs were obtained before and after completion of each cycle of pamidronate infusions. Children whose symptoms failed to be controlled with NSAIDs for at least a month trial were treated with IV pamidronate at a dose of 1 mg/kg/day (maximum 60 mg/day) once per month for three months. Some patients were treated with additional cycles depending on clinical and radiographic responses. If the response to pamidronate was suboptimal or in the presence of a disease flare, patients were then switched to a tumor necrosis factor (TNF) blocker (either adalimumab or etanercept). A total of 88 WB-MRI studies were analyzed in the 32 patients included in the study. Eleven patients received more than one cycle of pamidronate treatment and thus completed more than one follow-up MRI examination (Supplementary Figure-1). All the post-treatment MRIs were done at an average period of 5 months after each cycle of pamidronate therapy. Demographic, pre- and post-treatment clinical, relevant laboratory data, and other therapy details were retrieved from our electronic database.

MRI Protocol:

All MRI studies were performed on a 1.5-T MRI system (Magnetom Avanto, Siemens, Erlangen, Germany), with a "WB-MRI CRMO" institutional protocol used for the evaluation of CRMO. All examinations were performed with a dedicated multichannel surface coil system and patient in the supine position with and their hands being held by the side of their body. Integrated multichannel surface coil system allowed for the contiguous scanning. All exams included T2 single short tau inversion recovery (STIR) coronal sequences at multiple stations covering the whole body from vertex to toes with the patient free-breathing. The coronal T2 STIR sequence was performed with the following parameters: Repetition time (TR) 3000 ms, echo time (TE) 60 ms, inversion time (TI) 165 ms, field of view (FOV) 400–500 mm, matrix 380 × 290, slice thickness of 5 mm with 1 mm gap, number of signal averages (NEX) 6, echo train length (ETL) 26, and pixel bandwidth 446 Hz. The approximate scan time for each station was 5 min. The T2 STIR sagittal sequence of the spine was acquired at two stations and the time for each station was 5 min. The total scan time varied from 35 to 40 min depending on the child's height.

MRI assessment:

Before the study, two pediatric MSK radiologists (J.S. and J.P.) with more than five years of experience in reading musculoskeletal MRI were familiarized with the MRI scoring protocol, in a trial involving 10 patients which were not part of the study. Both the MSK radiologists are also members of an international CNO working group. Each radiologist independently interpreted and scored the MRIs using a standard picture archiving and communication system (PACS) workstation (GE Medical Solutions) in random order blinded to clinical and treatment details.

a) **Selection of anatomical locations for assessment:** We grouped the locations into the head (skull, mandible), shoulder girdles (clavicle, scapula), thorax (sternum, ribs), upper (humerus, radius, and ulna) and lower (femur, tibia, and fibula) extremities, hand (carpals, metacarpals, phalanges), feet (tarsals, metatarsals, phalanges), pelvis (ilium, sacrum, coccyx, periacetabulum and ischium and/pubis) and spine (from C1 to L5 vertebrae). For the scoring purpose, all the long tubular bones of the upper and

lower limb were divided into 3 main regions: proximal epimetaphysis, diaphysis, and distal epimetaphysis. The lesions of the bones of the hands and feet were counted and scored by the number of involved bones. The head region consisting of the right and left halves of the skull and mandible, shoulder girdle including each side of the clavicle and scapula, right and left-sided ribs, sternum, vertebrae from C1 to L5, each side of the sacrum and iliac bones, coccyx, right and left-sided periacetabular and ischium and/pubis bone segments were considered as one region and scored. Additionally, the presence and absence of the involvement of the posterior element of the spine were recorded and scored.

b) **Definitions and grading of item selection for the selected locations:** The diagnostic item selection and definition were decided based on the previously published MRI-based definitions in CNO and Spondyloarthritis Research Consortium of Canada scoring system for sacroiliitis studies[26,27,35,36]. Bone lesions were defined as abnormal hyperintensity of the bone marrow on STIR images compared to surrounding normal marrow. The presence of hyperintensity in the surrounding soft tissue was also recorded as soft tissue inflammation. Bone marrow signal size, signal intensity, adjacent soft tissue high signal, and bone expansion were selected as the key pathologic items for scoring the CNO lesions. Images were evaluated for the presence of focal, high-signal intensity in all STIR sequences. Subsequently, these marrow signal abnormalities at all the relevant anatomic locations were analyzed and scored for size and signal intensity, presence of soft tissue hyperintensity and bony expansion or collapse (in the spine) as shown in Figures-1-3, which were further graded/scored as shown in the data collection sheet, supplementary Table-1. The worst /highest signal intensity of bone marrow was recorded in the area of involvement/or the given bone segment as shown in Figure 1. The scoring of signal size was conducted based on the percentage of the whole segment of bone evaluated on the images after reviewing all images by scrolling back and forth on PACS.

Clinical assessment:

There are no standard or specific outcome measures to assess the clinical disease burden in patients with CNO. In this study, all patients were evaluated for bony tenderness and swelling and the number of affected CNO sites was recorded. All available surrogate clinical outcome measures were retrieved and analyzed pre and post-treatment, which included presence or absence of bone pain, localized swelling, arthritis, rash, enthesitis, uveitis, systemic symptoms (fever, weight loss, fatigue, and gastrointestinal symptoms) and visual analogue scale (VAS) score for pain. Laboratory parameters including serum calcium, alkaline phosphatase, C-reactive protein, erythrocyte segmentation rate, serum C-telopeptide (ng/L), and bisphosphonate pamidronate treatment details were recorded as shown in Supplementary Table-2.

Statistical analysis:

Descriptive analysis was performed to assess the prevalence of CNO lesions at each proposed anatomical region. Any bone region (defined as per Supplementary Table-1) to which a score of 1 or more was given by either of the two observers on the first pre-treatment WB-MRI of the patient was counted to provide a sensitive estimate of the relative distribution of lesions. **For assessment of detection of** lesions, the inter-reader agreement was calculated using kappa coefficient (k), by dichotomizing the 0-4 and 0-2 ordinal grades to 0 and 1, collapsing all non-zero grades. **For the quantification of the lesion**, the inter-reader agreement was conducted on the non-zero grades using Kappa statistics. The inter-rater reliability was considered excellent if the k was >0.80, good if it was 0.61–0.80, moderate if 0.41–0.60 and poor if ≤ 0.40. A bootstrapping method with 1000 resampling iterations was used to determine the 95% confidence interval for the kappa coefficients. Correlation between the bone lesion signal size and signal intensity was calculated using Spearman correlation coefficients.

Responsiveness was calculated using standardized response mean (SRM), defined as the mean change score over the standard deviation of change score. The two scores from the two readers were averaged for each WB-MRI evaluation for pre- and post-treatment WB-MRI scores. All available treatment intervals of each patient were included for analysis. Absolute value of SRM was

interpreted as large effect if >0.8, moderate effect if 0.8-0.5, small effect if 0.5-0.2, and no effect if <0.2. Data analysis was performed using the SPSS version. In all analyses, P values <0.05 were considered statistically significant.

Results

Thirty-two patients were included in this study and baseline characteristics are summarized in Supplementary Table-2. The VAS score for pain was available for 19 of the 32 patients before and after their first cycle of pamidronate treatment. Median VAS score for pain pre-treatment was 3.6 (IQR = 0.7-5.6) and post-treatment was 0.9 (IQR = 0.1-3.8). The median within-patient change in the VAS score was -1.0 (IQR = -3.7-0.0), corresponding to an SRM of -0.52, indicating moderate effect size. Twenty-one (66%) patients received one cycle of pamidronate, 8 patients received two cycles, and 2 and 1 patients received third and fourth cycles respectively because of persistent symptomatic extensive disease including spinal lesions. Pre- and post-treatment WB-MRI examinations were obtained after each cycle in all except six patients (three pre- and post-treatment MRIs were available in five patients who had two cycles and five MRIs in one patient with three cycles of pamidronate) as described in Supplementary Figure-1. Thirty-one patients (96.8%) underwent a trial of NSAIDs as initial therapy, six patients (18.7%) received a short course of corticosteroid at initial presentation before confirmation of diagnosis. Three patients (9.3%) had a trial of biologic therapy for suspected juvenile idiopathic arthritis (JIA) before CNO diagnosis and three (9.3%) others received disease-modifying antirheumatic drugs (DMARDs). The results are reported below in three parts 1) prevalence of lesions; 2) reliability of MRI assessment scoring system; and 3) MRI responsiveness to pamidronate therapy. Treatment response was assessed separately according to one, two, three, and four pamidronate cycles in 32, 11, 3, and 1 patients respectively. Ten patients (31%) with radiological evidence of persistent disease or presence of disease flare were started on a TNF blocker (eight on adalimumab and two on etanercept) after the follow-up MRIs. One additional patient was commenced on etanercept for associated JIA.

1) Prevalence of lesions:

Most lesions demonstrated multifocal ill-defined bone marrow hyperintensity on STIR images which were typically situated in the metaphyseal and epiphyseal regions adjacent to a growth plate of tubular bones**.** On WB-MRI STIR sequences, a total of 387 bone lesions (including 108 hand and feet bone lesions) were detected in 32 patients on baseline MRI examinations, before treatment with pamidronate. Lower limb regions were most commonly affected and occurred in descending order in the distal tibial metaepiphysis (66%), proximal tibial metaepiphysis (50%), distal femur metaepiphysis (50%), and distal fibular metaepiphysis (31%). Upper extremity involvement was considerably less common affecting the distal ulnar and radial metaepiphysis in 20%. Among the axial sites, the sacrum (33%) was the most commonly affected site. The spine, clavicle, mandible, skull, sternum, and ribs were also involved to a variable extent. There was only one case of isolated coccygeal and ulnar diaphyseal involvement while no lesions were found in the fibular and radial diaphysis and proximal radial metaepiphysis within this cohort. The detailed distribution of lesions is shown in Supplementary Table-3.

High signal intensity within the surrounding soft tissues was observed in 47 lesions on the baseline studies (Supplementary Table-3), predominantly adjacent to tubular bones of lower limbs (26 of 640 locations examined in the legs), followed by pelvis (particularly along the periacetabular region), clavicle, mandible, and spine. The bony expansion was present in 11 studied regions in baseline WB-MRI, and typically seen with clavicle and mandible. The bone collapse in the spine was commonly seen in the thoracic spine (3/9 involved thoracic vertebrae).

2) Reliability of MRI assessment of lesions:

a) For the detection of the lesions:

Inter-reader agreement on the detection of bone marrow lesions was excellent for all the body regions, with kappa ranging from 0.93 to 1.00 as shown in Table-1. Soft tissue changes and bone expansion or collapse were too infrequently observed in this sample to estimate inter-reader agreement. Inter-reader reliability of detection of bone marrow lesions, soft tissue lesions, bone expansion or collapse (in the spine), and posterior element involvement (in spine lesion) scores were assessed based on the images from the first pre-treatment MRI of 32 patients. Confidence intervals are derived from 1000 bootstrap resampling. A lesion was counted if either of the two readers rated the bone region as non-zero for the specific finding.

b) For the quantification of the lesions:

There was excellent inter-reader agreement on both the quantification of size and signal intensity of bone lesions in the arms and legs. There was perfect agreement on the size quantification of bone lesions in the pelvis, but moderate agreement on the signal intensity assessment (Table-1). The perfect agreement was observed for both size and intensity in the 18 spine lesions observed. The perfect agreement was observed in the size of lesions in the shoulder girdle, with good agreement on signal intensity. Lesion counts were low in the head and thorax in these patients, precluding more precise agreement estimates.

3) Responsiveness of MRI detected lesions to Pamidronate:

Response to pamidronate therapy was quantified for the first pamidronate cycle for all 32 patients using SRM of the change in the size and intensity of the bone lesion signal, separated by the body region. The majority of the bone marrow lesions were seen in the upper and lower limbs and pelvis. After the first cycle of pamidronate, both the signal size and intensity of these lesions showed a small response to therapy in the shoulder girdle and the lower limb lesions, whereas, in lesions of the upper limb and pelvis, the treatment response was not significant for either of these features. Lesions in the spine showed the highest response to treatment (as shown in Figure-4), at a decrease of 0.987 SRM for the signal size, and 0.922 for signal intensity for the

20 lesions studied (Table-2). Responsiveness was high also in skull and thorax, although the number of observed lesions was low in these regions. After the first cycle, 96 of the 279 lesions resolved (34%), while in the subset of 11 patients who underwent two or more cycles, 76% of lesions resolved after the second cycle. Twenty-one (7.5%) lesions worsened and 46 (16.4%) new lesions developed after one cycle (in all 32 patients) and the number of worsened lesions reduced to 2 (2%) and new lesions to 14 (14.9%) after the second cycle in 11 patients (Supplementary Table-4).

Discussion:

CNO is a painful, autoinflammatory osteitis, which may have a protracted course over years and is managed using a variety of treatments including NSAIDs, non-biologic DMARDs, corticosteroids, bisphosphonates, and biologic agents. Recently, bisphosphonates have shown effective and rapid pain relief in pediatric patients with persistent CNO including improvement of bone lesions on serial MRIs[28]. Bisphosphonates act as analgesic agents inhibiting bone resorption and have anti-inflammatory properties as well[37]. They have been used in many bone disorders in adults and children associated with significant osteopenia[38].

Our study presented data on inter-reader agreement on the detection and quantification of bone lesions and MRI response to pamidronate in pediatric patients with CNO with ongoing disease activity despite anti-inflammatories. CNO lesions are most frequently seen to involve the metaepiphysis of tubular bones, the pelvic bones, the small bones of feet, the spine, and the clavicle in the present study and it is in agreement with the previous studies[14,39-41]. This study examined the efficacy of pamidronate by comparing the pre- and post-WB-MRI bone lesions in pediatric patients with CNO. Overall, pamidronate therapy led to a good response (using WB-MRI as an objective measurement of disease activity) with the resolution of the bony lesions on follow up MRI in 34% and 76% after one and two cycles of pamidronate therapy respectively. This is in concordance with prior studies that

demonstrated a similar response to pamidronate treatment[27,28,30]. Although 34% of lesions disappeared after one cycle of treatment, ongoing improvement with a substantial response (resolution of 76% of the lesion) noted on WB-MRI occurred after two cycles in 11 patients. Twenty-one patients had only one cycle of therapy with overall >50% of residual and 16% of new lesions being noted on WB-MRI despite good clinical response. These results highlight the importance of using WB-MRI in assessing subclinical disease and response to treatment which can help guide in treatment decisions. In the group of patients who received more than one cycle of pamidronate treatment, some lesions resolved/disappeared in between the cycles as evident on pretreatment MRI examinations for the next cycle, once again emphasizing the role of WB-MRI in quantifying CNO lesions.

Our study proposes a new MRI scoring tool for CNO lesions and shows excellent inter-reader reliability for detecting and quantifying the size of the CNO lesions conversely to signal intensity of the bone marrow lesion. In our study, the signal intensity of the lesion was less reliable than size as the grading of the signal was quite variable among readers and depended upon the windowing of the image while evaluating on PACS. To our knowledge, there is no prior study available in the literature against which the results of our study could be compared to concerning the intensity of bone marrow edema in assessing CNO lesions. Hence, this point should be further evaluated in future prospective studies. Lesions in the bones of the feet were more common than the hand which is in keeping with the predilection of disease to involve the lower limb. However, it could have been affected by the visibility/readability of lesions on WB-MRI. Dedicated sagittal STIR sequence separately through the right and left foot was included in our WB-MRI CNO protocol, however, hands were imaged as a part of coronal STIR station 3 (through the lower abdomen and pelvis) and seen at the periphery of the image. Hence, we may have missed lesions in this region due to poor visualization of bones of the hand.

In our cohort, spinal lesions showed an excellent response to pamidronate with SRM of 0.9 which is consistent with prior published studies that have found the almost equal efficacy of pamidronate to spinal disease[28-30,42-44].

Limitations:

There were several limitations applied to our study. Firstly, it is a retrospective study that may result in missing clinical details that were not acquired in a standardized manner including VAS score for pain. Secondly, there could have been the impact of initial non-pamidronate treatment (NSAIDs, DMARDs, steroids, and biologic) on treatment outcomes. Furthermore, interobserver variability in quantifying the intensity of bone marrow edema of the lesions was suboptimal and could be improved in the future by the utilization of an atlas to guide scoring. Further, during certain stages of skeletal maturation linear bands of increased STIR signal intensity are noted at the metaphysis of the long bones as part of a physiologic process. This information could be available in an atlas to avoid false-positive scoring in future studies. The lack of dedicated hand imaging in our protocol probably led to the underestimation of bone lesions in this location which can be addressed in future prospective studies by placing the hand on thighs for better visibility. Additionally, this study did not correlate the radiologic changes with clinical parameters of disease activity.

Conclusion:

In this study, the interobserver reliability for detecting pediatric CNO lesions on MRI was excellent. When experienced radiologists report MRI data on CNO, we can be confident that the detailed assessment of MRI for these bone lesions is reproducible. On the other hand, further tutorial tools should be developed to improve the reliability of assessment of the signal intensity of CNO lesions. Nevertheless, MRI is an important and clinically relevant quantification tool that can be used to determine disease activity, the extent of disease, including disease sites that may be clinically occult, monitoring treatment response, make treatment adjustments and follow-up.

References:

1. Surendra G, Shetty U. Chronic recurrent multifocal osteomyelitis: A rare entity. J Med Imaging Radiat Oncol 2015;59:436-44.
2. Ferguson PJ, El-Shanti HI. Autoinflammatory bone disorders. Curr Opin Rheumatol 2007;19:492-8.
3. Iyer RS, Thapa MM, Chew FS. Chronic Recurrent Multifocal Osteomyelitis: Review. AJR Am J Roentgenol 2011;196:S87-91.
4. Carr AJ, Cole WG, Roberton DM, Chow CW. Chronic multifocal osteomyelitis. J Bone Joint Surg Br 1993;75:582-91.
5. Schultz C, Holterhus PM, Seidel A, Jonas S, Barthel M, Kruse K, et al. Chronic recurrent multifocal osteomyelitis in children. Pediatr Infect Dis J 1999;18:1008-13.
6. Beretta-Piccoli BC, Sauvain MJ, Gal I, Schibler A, Saurenmann T, Kressebuch H, et al. Synovitis, acne, pustulosis, hyperostosis, osteitis (SAPHO) syndrome in childhood: a report of ten cases and review of the literature. Eur J Pediatr 2000;159:594-601.
7. Omidi CJ, Siegfried EC. Chronic recurrent multifocal osteomyelitis preceding pyoderma gangrenosum and occult ulcerative colitis in a pediatric patient. Pediatr Dermatol 1998;15:435-8.
8. Laxer RM, Shore AD, Manson D, King S, Silverman ED, Wilmot DM. Chronic recurrent multifocal osteomyelitis and psoriasis--a report of a new association and review of related disorders. Semin Arthritis Rheum 1988;17:260-70.
9. Vittecoq O, Said LA, Michot C, Mejjad O, Thomine J-M, Mitrofanoff P, et al. Evolution of chronic recurrent multifocal osteitis toward spondylarthropathy over the long term. Arthritis Rheum 2000;43:109-19.
10. Demharter J, Bohndorf K, Michl W, Vogt H. Chronic recurrent multifocal osteomyelitis: a radiological and clinical investigation of five cases. Skeletal Radiol 1997;26:579-88.
11. Roderick MR, Ramanan AV. Chronic recurrent multifocal osteomyelitis. Adv Exp Med Biol 2013;764:99-107.
12. Costa-Reis P, Sullivan KE. Chronic Recurrent Multifocal Osteomyelitis. J Clin Immunol 2013;33:1043-56.
13. Nemcova D, Koskova E, Macku M, Brejchova I, Hoza J, Schiller M, et al. Chronic recurrent multifocal osteomyelitis (CRMO): clinical features and outcome in 21 Czech and Slovak children. CLINICAL AND EXPERIMENTAL RHEUMATOLOGY CLINICAL & EXPER RHEUMATOLOGY VIA SANTA MARIA 31, 56126 PISA, ITALY; 2011. p. 391-391.

14. Khanna G, Sato TSP, Ferguson P. Imaging of chronic recurrent multifocal osteomyelitis. Radiographics 2009;29:1159—77.

15. Mandell GA, Contreras SJ, Conard K, Harcke HT, Maas KW. Bone scintigraphy in the detection of chronic recurrent multifocal osteomyelitis. J Nucl Med 1998;39:1778—83.

16. Fritz J, Tzaribatchev N, Claussen CD, Carrino JA, Horger MS. Chronic recurrent multifocal osteomyelitis: comparison of whole-body MR imaging with radiography and correlation with clinical and laboratory data. Radiology 2009;252:842-51.

17. Girschick HJ, Raab P, Surbaum S, Trusen A, Kirschner S, Schneider P, et al. Chronic nonbacterial osteomyelitis in children. Ann Rheum Dis 2005;64:279—85.

18. Jansson A, Renner ED, Ramser J, Mayer A, Haban M, Meindl A, et al. Classification of nonbacterial osteitis: retrospective study of clinical, immunological and genetic aspects in 89 patients. Rheumatology (Oxford) 2007;46:154—60.

19. Job-Deslandre C, Krebs S, Kahan A. Chronic recurrent multifocal osteomyelitis: five-year outcomes in 14 pediatric cases. Joint Bone Spine 2001;68:245—51.

20. Kerrison C, Davidson JE, Cleary AG, Beresford MW. Pamidronate in the treatment of childhood SAPHO syndrome. Rheumatology (Oxford) 2004;43:1246—51.

21. Schnabel A, Range U, Hahn G, Berner R, Hedrich CM. Treatment Response and Longterm Outcomes in Children with Chronic Nonbacterial Osteomyelitis. J Rheumatol 2017;44:1058-65.

22. Carpenter E, Jackson MA, Friesen CA, Scarbrough M, Roberts CC. Crohn'sassociated chronic recurrent multifocal osteomyelitis responsive to infliximab. J Pediatr 2004;144:541—4.

23. Guérin-Pfyffer S, Guillaume-Czitrom S, Tammam S, Koné-Paut I. Evaluation of chronic recurrent multifocal osteitis in children by whole-body magnetic resonance imaging. Joint Bone Spine 2012;79:616-20.

24. Darge K, Jaramillo D, Siegel MJ. Whole-body MRI in children: current status and future applications. Eur J Radiol 2008;68:289-98.

25. Merlini L, Carpentier M, Ferrey S, Anooshiravani M, Poletti P, Hanquinet S. Whole-body MRI in children: Would a 3D STIR sequence alone be sufficient for investigating common paediatric conditions? A comparative study. Eur J Radiol 2017;88:155-62.

26. Zhao Y, Chauvin NA, Jaramillo D, Burnham JM. Aggressive Therapy Reduces Disease Activity without Skeletal Damage Progression in Chronic Nonbacterial Osteomyelitis. J Rheumatol 2015;42:1245-51.

27. Roderick M, Shah R, Finn A, Ramanan AV. Efficacy of pamidronate therapy in children with chronic non-bacterial osteitis: disease activity assessment by whole body magnetic resonance imaging. Rheumatology (Oxford) 2014;53:1973-6.

28. Miettunen PM, Wei X, Kaura D, Reslan WA, Aguirre AN, Kellner JD. Dramatic pain relief and resolution of bone inflammation following pamidronate in 9 pediatric patients with persistent chronic recurrent multifocal osteomyelitis (CRMO). Pediatr Rheumatol Online J 2009;7:2.

29. Hofmann C, Wurm M, Schwarz T, Neubauer H, Beer M, Girschick H, et al. A standardized clinical and radiological follow-up of patients with chronic non-bacterial osteomyelitis treated with pamidronate. Clin Exp Rheumatol 2014;32:604–9.

30. Bhat CS, Roderick M, Sen ES, Finn A, Ramanan A. Efficacy of pamidronate in children with chronic non-bacterial osteitis using whole body MRI as a marker of disease activity. Pediatr Rheumatol 2019;17:35.

31. Zhao Y, Sato TS, Nielsen SM, Beer M, Huang M, Iyer RS, et al. Development of CROMRIS (ChRonic nonbacterial Osteomyelitis MRI Scoring) Tool and Evaluation of its Interrater Reliability. J Rheumatol 2019 Oct 1.

32. Andreasen CM, Jurik AG, Glerup MB, Høst C, Mahler BT, Hauge EM, et al. Response to Early-onset Pamidronate Treatment in Chronic Nonbacterial Osteomyelitis: A Retrospective Single-center Study. J Rheumatol 2019 Apr 15.

33. Ramanan AV, Roderick MR, Shah R, Finn A. A75: Proposal of the Bristol Criteria for the Diagnosis of Chronic Non-bacterial Osteitis From a Cohort of 41 Patients. Arthritis Rheumatol 2014;66:S107.

34. Roderick MR, Shah R, Rogers V, Finn A, Ramanan AV. Chronic recurrent multifocal osteomyelitis (CRMO) - advancing the diagnosis. Pediatr Rheumatol Online J 2016;14:47.

35. Maksymowych WP, Inman RD, Salonen D, Dhillon SS, Williams M, Stone M, et al. Spondyloarthritis Research Consortium of Canada magnetic resonance imaging index for assessment of sacroiliac joint inflammation in ankylosing spondylitis. Arthritis Rheum 2005;53:703–9.

36. Panwar J, Tse S, Lim L, Tolend M, Radhakrishnan S, Salman M, et al. SPARCC (Spondyloarthritis Research Consortium of Canada) Magnetic Resonance Imaging Scoring System for Assessment of Sacroiliitis in Pediatric Patients with Juvenile Spondyloarthritis/Enthesitis Related Arthritis: A reliability, validity, and responsiveness study. J Rheumatol 2019;46:636-44.

37. Drake MT, Clarke BL, Khosla S. Bisphosphonates: mechanism of action and role in clinical practice. Mayo Clin Proc 2008;83:1032–45.

38. Munns CF, Rauch F, Travers R, Glorieux FH. Effects of Intravenous Pamidronate Treatment in Infants with Osteogenesis Imperfecta: Clinical and Histomorphometric Outcome. J Bone Miner Res 2005;20:1235-43.

39. Borzutzky A, Stern S, Reiff A, Zurakowski D, Steinberg EA, Dedeoglu F, et al. Pediatric chronic nonbacterial osteomyelitis. Pediatrics 2012;130:e1190–e11e7.

40. Schnabel A, Range U, Hahn G, Siepmann T, Berner R, Hedrich CM. Unexpectedly high incidences of chronic non-bacterial as compared to bacterial osteomyelitis in children. Rheumatol Int 2016;36:1737–1745.

41. Girschick HJ, Zimmer C, Klaus G, Darge K, Dick A, Morbach H. Chronic recurrent multifocal osteomyelitis: what is it and how should it be treated? Nat Clin Pract Rheumatol 2007;3:733–738.

42. Wipff J, Costantino F, Lemelle I, Pajot C, Duquesne A, Lorrot M, et al. A large national cohort of French patients with chronic recurrent multifocal osteitis. Arthritis Rheumatol 2015;67:1128–37.

43. Hospach T, Langendoerfer M, von Kalle T, Maier J, Dannecker GE. Spinal involvement in chronic recurrent multifocal osteomyelitis (CRMO) in childhood and effect of pamidronate. Eur J Pediatr 2010;169:1105–11.

44. Gleeson H, Wiltshire E, Briody J, Hall J, Chaitow J, Sillence D, et al. Childhood chronic recurrent multifocal osteomyelitis: pamidronate therapy decreases pain and improves vertebral shape. J Rheumatol 2008;35:707–12.

Figure and table legends:

Supplementary Figure-1 Flow diagram shows the case selection process, details of pamidronate cycles and treatment received before and after pamidronate therapy. WB-MRI=Whole body magnetic resonance imaging; NSAIDS=Non-steroidal anti-inflammatory drugs; DMARDS= Disease-modifying antirheumatic drugs; TNF=Tumor necrosis factor; IBD=Inflammatory bowel disease; JSpA= Juvenile spondyloarthritis.

Figure-1 Grading of severity of different items used for assessment of CNO lesions of long tubular bones. The items (bone marrow signal size, signal intensity, adjacent soft tissue high signal and bone expansion) were analyzed using the proposed grading system. Coronal T2 STIR images obtained through the distal tibiae in five different patients are shown. A, A 13-year-old boy with no bone marrow signal changes resulting in a bone marrow signal size score of 0; B, A 10-year-old girl with bone marrow signal size scored as grade 1 (<25 % of distal epimetaphysis segment of the tibia); C, A 11-year-old girl with bone marrow signal size scored as grade 2 (25-49 % of epimetaphysis). D, 12-year-old boy with bone marrow signal size scored as grade 3 (50-74% of epimetaphysis); E, 9-year-old girl with bone marrow signal size scored as grade 4 (75-100% of epimetaphysis). The worst signal intensity of the involved bone segment was taken into consideration for the grading of signal intensity of the lesion as depicted in images C and E, where marrow signal intensity is equal to the signal of the adjacent ankle joint fluid and hence scored as grade 2. Note the presence of surrounding soft tissue high signal received a grade of 1 in images D and E. Hence the following scores were obtained: for A=0; B=1; C=2+2=4; D=3+1=4; E=4+2+1=7. CNO=chronic nonbacterial osteomyelitis; STIR= short tau inversion recovery.

Figure-2 Presence of bone expansion and bone collapse. A, Coronal T2 STIR image through the neck and chest in a 14-year-old boy with CNO demonstrates diffuse confluent marrow high signal and expansion of the medial half of right clavicle (long arrow) as compare to the normal contralateral clavicle (short arrow), accumulated an additional score of 1. B-C, Sagittal T2 STIR images of the thoraco-lumbar spine in a 15-year-old boy that show <50% collapse of the L3 vertebra received a score of 1 while >50% collapse of

the involved T9 vertebra (mainly in the central part) gets a score of 2. D, Sagittal T2 STIR image of the cervical spine in a 6-year old girl demonstrates completely flattened C5 vertebra (vertebra plana) receiving a score of 3. CNO= CNO=chronic nonbacterial osteomyelitis; STIR= short tau inversion recovery.

Figure-3 Examples of grading of different body regions for assessment of CNO lesion in different patients. A, Sagittal T2 STIR image of the cervicothoracic spine in a 13-year-old girl shows multifocal vertebral involvement. Scores for C5 (SS+SI+C+PE= 4+1+0+0) =5; T1 (4+2+0+1) =7; T2 (4+1+1+0) =6; T6 (4+1+0+0) =5 and T7 (1+1+0+0) =2. B, Coronal T2 STIR image of the pelvis in a 11-year-old girl shows a score of 7 (SS+SI+ST+BE= 4+2+1+0) for the right sided periacetabular lesion. Signal intensity (small black arrow) which is equal to the fluid in the urinary bladder receives a score of 2 while presence of soft tissue hyperintensity (long black arrow) gets a score of 1. The dotted line shows the watershed border between the iliac and periacetabular regions. Thus, the right iliac lesion receives a score of (2+1+1+0) 4. C, Coronal T2 STIR image in a 15-year-old girl depicts presence of focal marrow hyperintensity in the first metacarpal (short white arrow) receives a score of 1. Note that the iliac bone lesion (long white arrow) is also seen in the same patient. D-E, Sagittal images through the right foot in a 15-year-old boy receives a score of 3 for the three involved bones. The other items were not recorded for small bones of feet and hand. CNO=chronic nonbacterial osteomyelitis; STIR= short tau inversion recovery; SS=signal size; SI=signal intensity; C=collapse; PE=posterior element; ST=soft tissue; BE=bone expansion.

Figure-4 Pre- and post-pamidronate WB-MRI. A, Sagittal STIR whole spine image before pamidronate therapy shows marrow high signal involving the C5, T1, T2, T6, T7, T9, T10 and L1 vertebral bodies consistent with vertebral lesions. The total score of the vertebral lesions dropped from 45 to 11 after one cycle of pamidronate was administered to patients as seen on post-treatment STIR sagittal spine image, B consistent with considerable response to treatment. WB-MRI=whole body-magnetic resonance imaging; STIR= short tau inversion recovery.

Supplementary Table-1 Data collection sheet for Whole-Body MRI Scoring System used for quantifying the CNO Lesions in this study. CNO=chronic nonbacterial osteomyelitis.

Supplementary Table-2: Baseline demographic, clinical, laboratory data and treatment details from the patients included in this study.

Supplementary Table-3: Prevalence of CNO lesions on first pre-treatment WB-MRI for all 32 patients. This prevalence of bone marrow involvement for each of the bone was calculated because each patient received a single score for each of the bone-region. CNO=chronic nonbacterial osteomyelitis.

Table-1: Inter-reader agreement on the detection and assessment of the size and signal intensity of bone marrow lesions on the first pre-treatment MRI of 32 pediatric patients with CNO. CNO=chronic nonbacterial osteomyelitis.

Table-2: Response to the treatment in axial and appendicular lesions in 32 patients during first cycle of pamidronate as measured by WB-MRI.

Supplementary Table-4: Treatment response of WB-MRI lesions to Pamidronate. This frequency table does not include hands and feet bone lesions, because the hand and feet lesions were not tracked per lesion over time in contrast to the remainder.

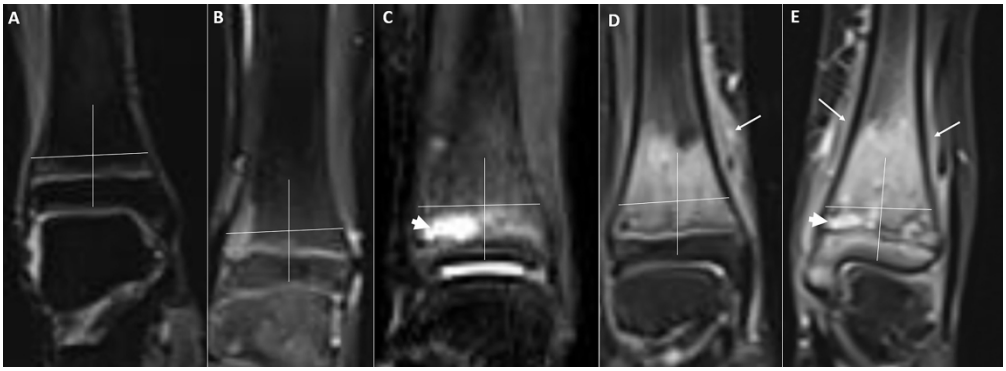

Figure 1.

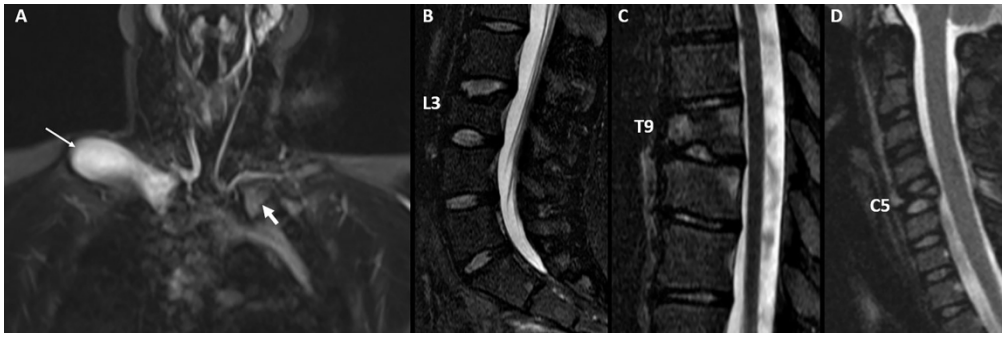

Figure 2.

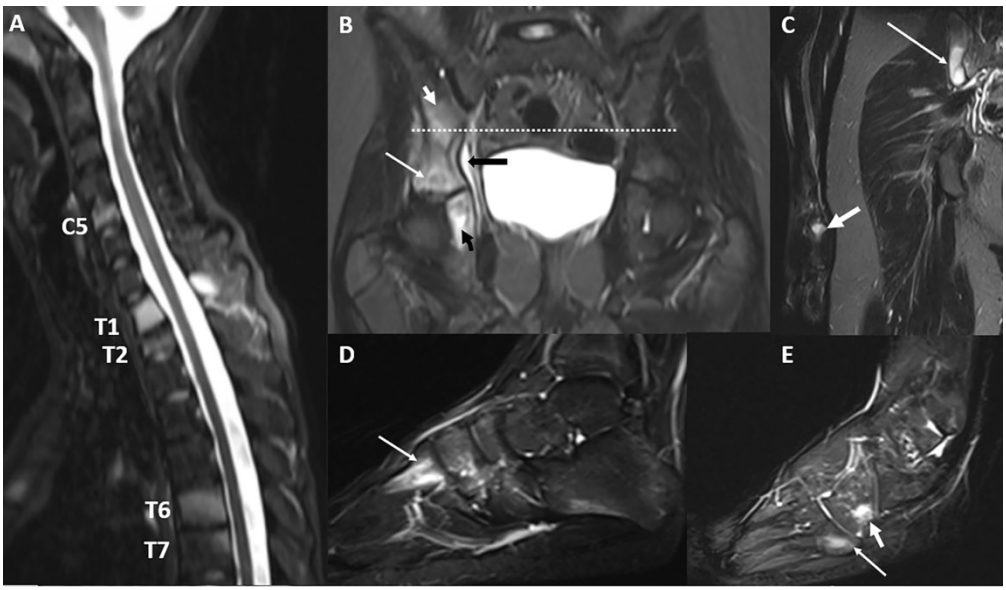

Figure 3.

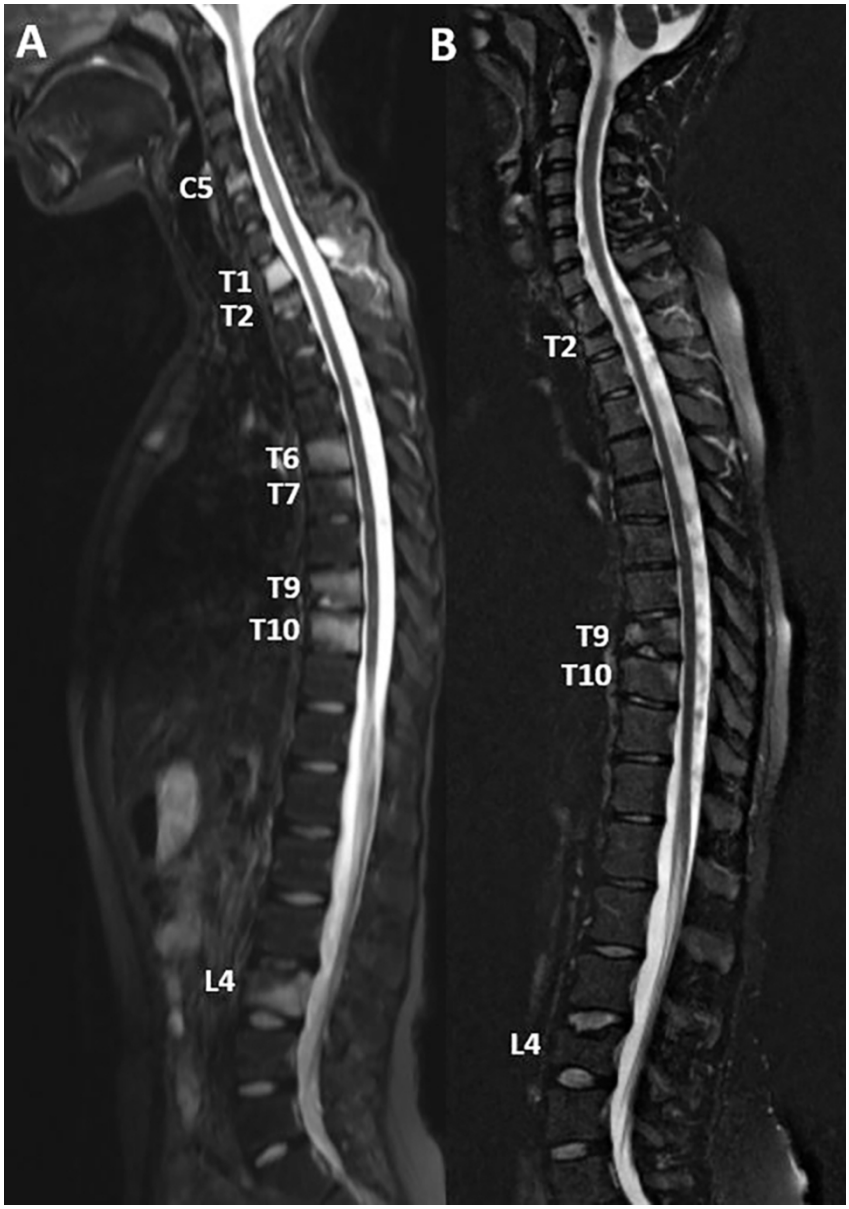

Figure 4.

	N of regions examined	Bone marrow lesions [Kappa, (95% CI)]				Soft tissue hyperintensity		Bone expansion/collapse*	
		N	Presence	Signal size	Signal intensity	N	Kappa, (95% CI)	N	Kappa, (95% CI)
Head	128	6	1.00 (1.00-1.00)	.76 (.36-1.00)	.57 (.00-1.00)	2	1.00 (1.00-1.00)	2	.80 (.00-1.00)
Shoulder girdle	128	13	.96 (.85-1.00)	.88 (.56-1.00)	.60 (.18-1.00)	4	1.00 (1.00-1.00)	3	1.000 (1.00-1.00)
Thorax	96	4	1.00 (1.00-1.00)	-	.00 (-.60-1.00)	0	-	0	-
Pelvis	288	45	.97 (.94-1.00)	.92 (.79-1.00)	.47 (.21-.70)	7	.75 (.00-1.00)	1	.50 (.00-1.00)
Upper limbs	576	38	.93 (.86-.99)	.65 (.44-.83)	.61 (.36-.82)	1	1.00 (1.00-1.00)	1	1.00 (1.00-1.00)
Lower limbs	640	155	.98 (.96-1.00)	.80 (.71-.87)	.75 (.64-.85)	26	.82 (.66-.93)	4	.72 (.33-1.00)
Spine	768	18	.97 (.90-1.00)	.88 (.63-1.00)	.83 (.29-1.00)	2	1.00 (1.00-1.00)	5	.80 (.00-1.00)

Table-1 Inter-reader agreement on the assessment of bone and soft tissue CNO lesions on the first pre-treatment WBMRI exam from 32 pediatric patients with CNO. *Bone collapse is measured for spine, whereas bone expansion is measured for other regions.

Bone Region	Total locations examined	Lesion Signal Size		Lesion Signal Intensity		Bone region	Total hands/ feet examined	No of hands/feet with one or more lesions in pre/ posttreatment MRI	SRM
		N of involved locations in pre or post	SRM	N of involved locations in pre or post	SRM	Hand	64	4	-0.614
Head (skull, mandible)	128	6	-0.645	6	-0.598	Feet	64	45	-0.210
Shoulder girdle (clavicle, scapula)	128	16	-0.412	16	-0.530				
Thorax (sternum, ribs)	800	4	-0.866	4	-1.095				
Pelvis (hip bones, sacrum, coccyx)	288	59	-0.193	59	-0.019				
Arms (humerus, radius, ulna)	576	54	-0.194	54	-0.341				
Legs (femur, tibia, fibula)	640	183	-0.325	183	-0.244				
Spine (C1 to L5 vertebrae)	768	20	-0.987	20	-0.922				

Table-2 Response to the treatment in axial and appendicular lesions in 32 patients during the first cycle of pamidronate as measured by WB-MRI. The response to hands and feet bone lesions is mentioned separately, because the hand and feet lesions were not tracked per lesion over time in contrast to the remainder.